

Characterization of adenosine receptor in its native environment: insights from molecular dynamics simulations of palmitoylated/glycosylated, membrane-integrated human A_{2B} adenosine receptor

Mahboubeh Mansourian · Armin Madadkar-Sobhani · Karim Mahnam · Afshin Fassihi · Lotfollah Saghaie

Received: 16 December 2011 / Accepted: 3 April 2012 / Published online: 9 May 2012
© Springer-Verlag 2012

Abstract Selective A_{2B} receptor antagonists and agonists may play a role in important pathologies such as gastrointestinal, neurological (i.e., Alzheimer disease and dementia) and hypersensitive disorders (i.e., asthma), diabetes, atherosclerosis, restenosis and cancer. Hence, it is regarded as a good target for the development of clinically useful agents. In this study, the effects of lipid bilayer, N-acetylglucosamine and S-palmitoyl on the dynamic behavior of A_{2B}AR model is explored. Homology modeling, molecular docking and molecular dynamics simulations were performed to explore structural features of A_{2B}AR in the presence of lipid bilayer. Twenty ns MD simulation was performed on the constructed model inserted in a hydrated lipid bilayer to examine stability of the

best model. OSIP339391 as the most potent antagonist was docked in the active site of the model. Another MD simulation was performed on the ligand-protein complex to explore effects of the bilayer on this complex. A similar procedure was performed for the modified protein with N-acetylglucosamine and S-palmitoyl moieties in its structure. Phe173 and Glu174 located in EL2 were determined to be involved in ligand-receptor interactions through π - π stacking and hydrogen bonding. Asn254 was crucial to form hydrogen-bonding. The reliability of the model was assessed through docking using both commercial and synthetic antagonists and an r^2 of 0.70 was achieved. Our results show that molecular dynamics simulations of palmitoylated/glycosylated, membrane-integrated human A_{2B}AR in its native environment is a possible approach and this model can be used for designing potent and selective A_{2B}AR antagonists.

Electronic supplementary material The online version of this article (doi:10.1007/s00894-012-1427-y) contains supplementary material, which is available to authorized users.

M. Mansourian · A. Fassihi (✉) · L. Saghaie
Department of Medicinal Chemistry, School of Pharmacy and
Isfahan Pharmaceutical Sciences Research Center, Isfahan
University of Medical Sciences,
Isfahan, Iran
e-mail: fassihi@pharm.mui.ac.ir

A. Madadkar-Sobhani
Department of Bioinformatics, Institute of Biochemistry and
Biophysics (IBB), University of Tehran,
Tehran, Iran

A. Madadkar-Sobhani (✉)
Life Sciences Department,
Barcelona Supercomputing Center (BSC),
08034 Barcelona, Spain
e-mail: amadadka@bsc.es

K. Mahnam
Biology Department, Faculty of Science, Shahrekord University,
Shahrekord, Iran

Keywords A_{2B}AR · GPCR · Molecular docking · Molecular dynamics simulation · Post-translational modifications

Introduction

Adenosine is an endogenous purine nucleoside widely distributed in mammalian tissues. The first recorded report describing evidence for an adenosine receptor dates back to 1976. Up to now four adenosine receptor (AR) subtypes, A₁, A_{2A}, A_{2B}, and A₃ have been characterized. The A_{2A}AR and A_{2B}AR stimulate adenylyl cyclase through coupling to the G_s protein resulting in an increase in cyclic adenosine mono phosphate (cAMP) levels, whereas the A₁ and A₃ subtypes inhibit adenylyl cyclase via coupling to G_i protein thus leading to diminishment of cAMP. Growing evidence

has indicated that agonists and antagonists of these receptors may have a variety of potential therapeutic applications although the rational design of new analogs seems to be a partially difficult task because their three-dimensional crystal structures are not available yet [1–4]. Adenosine receptors belong to the superfamily of G-protein coupled receptors (GPCRs), a large family of very successful drug targets [1]. A GPCR is characterized structurally by the presence of a bundle consisting of seven hydrophobic α -helical segments (TM1–TM7). This bundle has approximately 25 residues in length, each traversing the lipid bilayer, followed by one short membrane-associated helix (TM8). Transmembrane domains are connected by nonhelical loops through six alternating extracellular (EL 1–3) and intracellular loops (IL 1–3) at the inner and outer face of the membrane. The helices are placed in a lipid environment, while the loop regions are surrounded by an aqueous medium. The N-terminus is located on the extracellular side of the membrane, whereas the C-terminus region is placed on the intracellular side [1, 5].

The function of a protein is often strongly affected by post-translational modifications (PTMs) which occur on almost all proteins analyzed to date [6]. Glycosylation, palmitoylation, disulfide linkage formation, terminal amino acid acylation and phosphorylation are some examples of PTMs. For GPCRs, these changes account for differences in G protein coupling and ligand affinity [7].

Many GPCRs have one or more conserved cysteine residues localized at the C-terminal end of the cytoplasmic helix 8 covalently [8] attached to one or more lipids [9]. Dynamic palmitoylation has been demonstrated to occur on one or more of these cysteines of several G-protein-coupled receptors, including bovine rhodopsin, β_2 and α_{2A} adrenergic and D_1 dopamine [10]. One or more consensus palmitoylation sites can be observed in all of the AR subtypes, except the A_{2A} [11]. No role for putative A_{2B} AR palmitoylation has been described because no site directed mutagenesis has been performed for this subtype [12]. This post-translational modification may be important for the function of G protein-coupled receptors. This is deduced by the fact that the presence of Cys residues susceptible to palmitoylation is highly conserved among these proteins [13].

Glycosylation is the most extensive posttranslational modification made to numerous proteins of cellular membranes with diverse functions [14]. Glycosylation in EL2 has been confirmed for some subtypes of adenosine receptors. A_1 , A_{2A} and A_{2B} are among the adenosine receptors that have consensus sites for N-linked glycosylation in EL2 [15].

Like most other transmembrane GPCRs, the A_{2B} AR crystal structure has not been obtained to date. Several studies have been reported on prediction of the A_{2B} AR binding site. Ivanov et al. reported a structural model of

A_{2B} receptor based on the crystal structure of the bovine rhodopsin, which only shared 23 % sequence identity [16]. While, the recently published crystal structure of the hA_{2A} , which shared 61 % identity with hA_{2B} , in complex with the high affinity antagonist ZM-241385, provides a new template for A_{2B} modeling [17]. Sherbiny et al. built the A_{2B} homology model based on X-ray structures of bovine rhodopsin, the β_2 -adrenergic receptor, and the A_{2A} AR and proposed a common binding site for antagonists and agonists [18]. Another prediction for the 3D structure of adenosine receptors was reported by Goddard et al. They observed the subtype selectivity using the so-called GEN-SEMBLE method [19]. The binding modes of A_{2B} AR antagonists are also demonstrated by Cheng et al. using ligand-based and receptor-based methods [20]. Analysis of the subtype-specific ligand-receptor interactions allowed identification of the major determinants of ligand selectivity by Katritch et al. [8]. Very recently, Rodríguez et al. performed an all-atom MD simulation of apo form of both A_{2A} AR and homology modeled A_{2B} AR [21].

A common shortcoming shared by the above-mentioned studies is that the authors explored A_{2B} structure/function without considering the influence of lipid bilayer (one exception is Rodríguez et al. study) and PTMs on its folding. In this study, the effects of lipid bilayer, N-acetylglucosamine and S-palmitoyl on the dynamic behavior of A_{2B} model is explored. The possible binding modes of the most potent antagonist, i.e., OSIP339391 [22], in the state close to A_{2B} natural conditions is also characterized. State of the art homology modeling, molecular dynamics simulation and docking are exploited to achieve the best results.

Methods

A_{2B} model building using homology modeling method

Homology modeling of A_{2B} AR was normally performed along a series of well-defined and commonly accepted steps as follows:

The primary sequence of the human A_{2B} AR was downloaded from UniProt, which contains 332 amino acids (UniProtKB/Swissprot: P29275). Using Basic Local Alignment Search Tool (Blast) available at NCBI, crystallography structure of A_{2A} (PDB ID: 3EML) [17] was selected as the template with a high sequence identity (61 %) with A_{2B} [23]. Blast results of A_{2B} and A_{2A} showed the score of 78.2 and E value of 5×10^{-15} . Multiple sequence alignment (MSA) was performed between the target and the template receptors from 22 mammalian species using T-COFFEE to obtain an alignment with higher sequence identity with the target receptor.

Alignment derived by MSA was employed to build homology models of A_{2B} (Supplementary Fig. S1). Three-dimensional models containing all non-hydrogen atoms were obtained automatically using MODELLER (9v5) [24]. From the 1000 models generated by MODELLER, the one corresponding to the lowest value of the probability density function (pdf) and the fewest restraint violations was selected for the loop refinement stage. Inspection of the template structure revealed that loop 149–155, one of the functionally most important parts of the A_{2A}AR, is disordered and is not present in the PDB structure (missing residues). The higher conservation seen in TM regions, however, is responsible for the similar overall folding of the members of GPCRs. Modeling of the extracellular regions of GPCR is challenging because of limited homology with known structures and because of limitations of current loop modeling techniques [24]. The problematic region in the model of the A_{2B} was EL2 (147–167), which was subjected to *ab initio* loop modeling procedure [25] implemented in the MODELLER. Discrete optimized protein energy (DOPE) was used to assess the energy and the quality of the 10,000 models generated [26].

Stereochemical quality assessment of the models and the generation of the Ramachandran plot have been carried out through PROCHECK [27]. The root mean square deviations (RMSDs) of the models relative to the template were calculated using MODELLER. Verify-3D (structure evaluation server) was employed from its web server (<http://www.doe.mbi.ucla.edu/verify3d.html>) [28].

Docking studies for the selected antagonists

OSIP339391 is a novel, selective and high affinity ligand that can be a useful tool in further exploration of ligand interaction with A_{2B}AR active site [22]. The starting structure of the antagonist was built and optimized using Hyperchem 7.0 (HyperCube Inc., Gainesville, FL).

AutoDockTools [29] was used to generate both grid and docking parameter files. The docking studies were performed by AutoDock software version 4.2. Since the location of the ligand in the complex was known, the maps were centered on the binding site of ligand on C α of Asn254. This residue was selected according to the available data from literature and site-directed mutagenesis [30]. Grid points of 96 \times 80 \times 70 separated by 0.375 Å in each dimension were applied. At the end of docking experiment with 200 runs, a cluster analysis was performed. The 200 independent docking conformations were clustered according to a 2.0 Å RMSD criterion and were ranked according to the binding free energy.

LIGPLOT program was used to investigate the hydrophobic and hydrogen bonding interactions between the ligand and receptor [31].

Molecular dynamics simulations

Molecular dynamics simulations were performed to relax the modeled system. GROMACS 4 package [32] was used with ffgmx force field (Gromos87) at constant temperature and pressure. To mimic the membrane environment, the best model obtained from the model output was inserted manually into the center of a lipid bilayer consisting of 340 molecules of POPE (palmitoylcholine phosphatidyl ethanolamine) lipid bilayer. The lipid bilayer was described using a previously developed topology file for lipid molecules [33]. The α -helices were modulated manually perpendicular to *x-y* plane of the lipid bilayer by VMD 1.8.5 program [34]. Overlapping protein-lipids were removed using InflateGro script. The embedded A_{2B}AR together with the POPE molecules were positioned in a box with the dimensions of 96 \times 95 \times 100 Å and solvated using a simple point charge (SPC216) water model [35]. Overlapping lipid and water molecules were removed. Chloride ions were added into the box to obtain neutralized system and periodic boundary conditions were applied. Then, energy minimization was carried out for the system using the steepest descent algorithm. After energy minimization using a steepest descent method, the system was subject to equilibration at 323 K and normal pressure for 1 bar under the conditions of position restraints for heavy atoms of 1000 kJ mol⁻¹ nm⁻¹ and LINCS constraints for all bonds (even heavy atom-H bonds). The final MD calculations were performed under the same conditions except that the position restraints were removed. An NVT ensemble of 1 ns was adopted at constant temperature of 323 K and with a coupling constant of 0.1 ps. After stabilization of temperature an NPT ensemble of 2 ns was performed. In this phase a constant pressure of 1 bar was employed with a coupling constant of 5 ps [36]. The coupling scheme of V-rescale as modified Berendsen thermostat was employed for NVT ensemble. The Nosé-Hoover thermostat in membrane simulations at the beginning of NPT and the production phase of MD was used. The particle mesh Ewald (PME) method interaction and the LINCS algorithm for covalent bond constraints were used. MD time step was set to 2 fs [37, 38].

MD simulations were performed in four stages as follows:

Stage I: The final A_{2B}AR model derived from homology modeling process was subjected as starting structure to 20 ns of MD simulation. The system in this stage was comprised of 54,503 atoms including 13,094 water molecules, 233 POPE molecules, A_{2B}AR and six chloride ions. Ligand (OSIP339391), with one of its two nitrogen atoms in the piperazine ring protonated, was docked into the conformation of A_{2B}AR obtained from MD simulation in stage I. The conformation with the lowest binding free energy of the

ligand was selected as the initial conformation for 20 ns MD simulation in the next stage.

Stage II: Parameters of the ligand were obtained from the PRODRG server [39]. MD simulation in this stage generated orientations of the ligand in the putative binding pocket of A_{2B} resulting in the stable model of A_{2B}-ligand complex.

Stage III: A_{2B}AR was subjected to PTMs. Certain types of modifications affect only specific amino acid residues. Such patterns are, for example, listed in the PROSITE database (<http://www.expasy.org/prosite/>) and also web servers such as <http://www.cbs.dtu.dk/services/NetNglyc/>. Based on the information available at the above mentioned web servers and literature [11, 15, 40], A_{2B}AR has been shown to be palmitoylated on Cys311 and glycosylated on Asn153 and Asn163. The optimized structure of the N-acetylglucosamine and palmitoylic acid were obtained using Hyperchem. The carbohydrate was attached at its anomeric carbon through a β -N-glycosidic linkage (N-linked), involving the amide nitrogen of asparagine and N-acetylglucosamine as the terminal sugar (GlcNAc-Asn) [41].

Parameters for the N-acetylglucosamine and S-palmitoyl were obtained by the PRODRG server. Point charges for N-acetylglucosamine and S-palmitoyl bound to Asn and Cys residues were obtained from a B3LYP/6-31 G* calculation using the chelpg charge fitting procedure using Gaussian 98 [42]. Then, 20 ns MD simulation was performed on the constructed A_{2B}AR model inserted in a hydrated lipid bilayer in the presence of N-acetylglucosamine (GlcNAc) and S-palmitoyl. The protocol of MD simulation was the same as the one used for the simulation of free A_{2B} described above. The ligand was docked into the modified receptor structure obtained in stage III.

Stage IV: 20 ns MD simulation was performed on the resulting ligand-protein complex. Here again, the utilized system was the same as the previous stage.

Virtual screening

To find the possible ligand binding conformation of A_{2B}, 41 ligands (Table 1) were docked into the structure of A_{2B}AR at the end of stage IV simulation using the same molecular docking procedure mentioned in the *docking studies* section. Integrated scoring function of AutoDock, based on the empirical binding free energy was used for the binding affinity prediction.

The first 39 compounds were selected as synthesized A_{2B} antagonists [43] based on their good correlation in

a QSAR study carried out by authors. OSIP339391 [22] and CVT6883 [44] were included as the most potent and the most selective A_{2B} antagonist, respectively. These compounds have some common structural features: a pyrrolopyrimidine ring, a piperazine ring, carbonyl group and phenyl moieties in the middle and end positions with various side chains (arms).

The inhibition constant (K_i) of the cluster with the lowest free energy of binding reported by AutoDock for each ligand that at the same time had a similar position and orientation with OSIP339391 at the end of stage IV simulation, was used for the correlation with the experimental binding affinities. Predicted and experimental K_i s were converted to pK_i by the $pK_i = -\log(K_i)$ formula.

Results

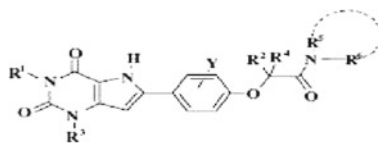
Homology modeling

Although homology modeling has been extensively performed in the case of GPCRs, this technique faces several limitations for these receptors, including poor sequence identity between target and template sequences, and the limited number of structural templates (only six at the time of this writing) [20, 45]. This emphasizes the need for incorporating available experimental information such as site-directed mutagenesis and structure-activity relationships data along with homology modeling for developing acceptable 3D models for GPCRs.

One of the most important points in modeling the individual backbone of hydrophilic loops is the presence of the disulfide bond between TM3 and EL2, which is highly conserved among all rhodopsin-like receptors [46]. A conserved disulfide bond, found in all adenosine receptors, is formed in the extracellular domain of the A_{2B} receptor between Cys78 (at the top of TM3) and Cys171 (located in EL2). This disulfide bond was made and kept as a constraint in the homology model building [17].

The quality of the resulted model was checked using PROCHECK. Ramachandran plot showed that more than 98.0 % of the ϕ/ψ angles of the residues are located in the favored regions (Fig. S2). The G-factors were 0.2 °, -0.1 ° and 0.07 ° for dihedrals, covalent and in overall, respectively. The overall main-chain and side-chain parameters, as evaluated by PROCHECK, are all very favorable. Therefore, according to PROCHECK the optimized model showed relatively good protein geometry, and most of the quality parameters were better than average or in the range of tolerance default (thresholds).

To study the orientation of A_{2B}AR helices, we superimposed the transmembrane regions of the model with the

Table 1 Chemical structures, experimental and predicted binding affinities at the hA_{2B} AdoR of 1,3-dialkyl-9-dAX piperazinamides (1–39), OSIP339391 and CVT-6883 antagonists

Compound	R ¹ /R ²	R ³ /R ⁴	NR ⁵ R ⁶	Y	Experimental pKi	Predicted pKi	Ref
1	CH ₃ /CH ₃	H/H		H	8.55	8.31	[43]
2	CH ₃ /CH ₃	H/H		H	8.47	8.64	[43]
3	CH ₃ /CH ₃	H/H		H	8.46	8.29	[43]
4	CH ₃ /CH ₃	H/H		H	8.38	8.64	[43]
5	CH ₃ /CH ₃	H/H		H	8.20	7.71	[43]
6	CH ₃ /CH ₃	H/H		H	8.20	8.25	[43]
7	CH ₃ /CH ₃	CH ₃ /H		H	8.09	7.80	[43]
8	CH ₃ /CH ₃	H/H		H	8.02	7.96	[43]
9	CH ₃ /CH ₃	H/H		H	7.88	7.42	[43]
10	CH ₃ /CH ₃	H/H		H	7.56	7.67	[43]
11	CH ₃ /CH ₃	H/H		H	7.29	7.00	[43]
12	CH ₃ /CH ₃	H/H		H	7.27	7.31	[43]
13	CH ₃ /CH ₃	H/H		m-OCH ₃	7.24	7.64	[43]
14	CH ₃ /CH ₃	CH ₃ /H		H	7.15	7.38	[43]

A_{2A} crystal structure. The C α atom RMSD was 0.36 Å, confirming a high likelihood of having a model close to native structure.

The final structure has been further evaluated for overall quality by Verify3D. Prediction of torsion angle restraints for the side chains of the developed A_{2B} model using predictor had shown that the confidence score and the similarity score for almost all residues is above zero (Fig. S3). According to these evaluation methods the generated human A_{2B}AR model seems to be in good quality based on common structural criteria.

The sequence identity between A_{2A}AR and A_{2B}AR is 61 %. As higher similarity results in better modeling [24], it can be concluded that the obtained model possesses a high reliability based on the high sequence identity to A_{2A} crystal structure template.

Molecular dynamics simulation: stage I

It is commonly accepted that the most realistic and useful way for performing MD simulations of membrane proteins is the use of a phospholipid bilayer solvated by water

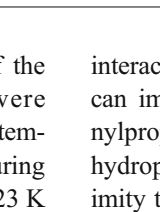
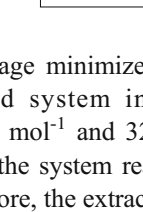
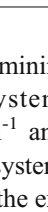
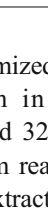
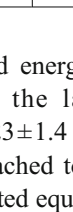
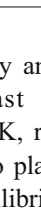
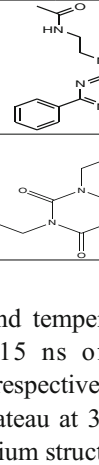
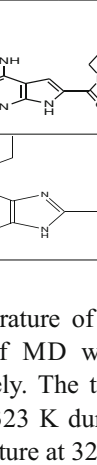
Table 1 (continued)

Compound	R ¹ /R ²	R ³ /R ⁴	NR ⁵ R ⁶	Y	Experimental pKi	Predicted pKi	Ref
15	CH ₃ /CH ₃	H/H		H	6.76	6.44	[43]
16	Pr/Pr	H/H		H	8.38	8.17	[43]
17	Pr/Pr	H/H		H	8.32	7.96	[43]
18	Pr/Pr	H/H		H	8.16	7.83	[43]
19	Pr/Pr	H/H		H	7.69	7.29	[43]
20	Pr/Pr	CH ₃ /CH ₃		H	7.61	7.44	[43]
21	Pr/Pr	H/H		H	7.41	7.01	[43]
22	Pr/Pr	H/H		H	7.00	7.45	[43]
23	CH ₃ /Pr	H/H		H	8.37	7.87	[43]
24	CH ₃ /Pr	H/H		H	8.22	7.89	[43]
25	(CH ₃) ₂ CHCH ₂ /Pr	H/H		H	8.13	7.99	[43]
26	Cypropyl-CH ₂ /Cypropyl-CH ₂	H/H		H	7.93	7.82	[43]
27	Pr/CH ₃	H/H		H	7.88	7.96	[43]
28	CH ₃ /Pr	H/H		H	7.83	7.44	[43]
29	CH ₃ CH ₂ /CH ₂ CH ₃	H/H		H	7.59	7.94	[43]
30	CH ₃ /Pr	H/H		H	7.59	7.83	[43]
31	CH ₃ /Pr	H/H		H	8.59	8.56	[43]
32	CH ₃ /Pr	H/H		H	8.25	7.96	[43]
33	CH ₃ /Pr	H/H		H	8.04	7.14	[43]

molecules. The lipid environment in the membrane can have a serious impact on the protein conformation [47], and it is not easy to obtain this final conformation via crystallography. Hydrophobic interactions between the nonpolar amino acids and the fatty acyl groups of the membrane lipids firmly anchor the protein in the membrane.

This stage of the study focuses on the biomembrane model of the protein in a pre-equilibrated native-like phospholipids bilayer environment, comprising A_{2B}AR and lipid bilayer at full hydration. MD simulations were performed to study the conformational variations and determine the stability of the obtained A_{2B}AR 3D structure within an explicit lipid environment.

Table 1 (continued)

Compound	R ¹ /R ²	R ³ /R ⁴	NR ⁵ R ⁶	Y	Experimental pKi	Predicted pKi	Ref
34	CH ₃ /CH ₃	H/H		H	8.02	7.99	[43]
35	CH ₃ /CH ₃	H/H		H	7.91	8.03	[43]
36	Pr/Pr	H/H		H	7.87	8.01	[43]
37	Pr/Pr	H/H		H	7.68	7.52	[43]
38	Pr/Pr	H/H		H	7.67	7.99	[43]
39	CH ₃ /CH ₃	H/H		m-OCH ₃	7.51	7.43	[43]
OSIP339391					9.38	9.23	[22]
CVT-6883					8.09	7.96	[44]

The average minimized energy and temperature of the investigated system in the last 15 ns of MD were $-922048 \text{ kJ mol}^{-1}$ and $323 \pm 1.4 \text{ K}$, respectively. The temperature of the system reached to plateau at 323 K during 1 ns. Therefore, the extracted equilibrium structure at 323 K belonging to the A_{2B} was obtained under stable temperature conditions. RMSD of the protein backbone was calculated and showed stabilization at 0.30 nm after 5 ns (Fig. 1a). In the last 15 ns of simulation, the system was fairly stable and did not alter meaningfully from $0.30 \pm 0.01 \text{ nm}$.

To explore the characteristic binding modes of A_{2B}AR ligand and to reveal the most essential residues involved in ligand recognition, molecular docking was performed on A_{2B}AR binding pocket. The conformation with the lowest free energy of binding change was selected as the starting structure for the next simulation.

Two-dimensional schematic representation of the best possible binding mode of OPIS339391 in the A_{2B}AR active site is depicted in Fig. 2a. The docking results showed hydrogen-bonding interactions with Ile65 and Ser68 in EL1 and aromatic interactions with Trp247, His251 in TM6, Ala64 in TM2, Leu69 in EL1 and Val85 in TM3 which accommodate the phenyl moiety of the ligand and π - π hydrophobic interactions with Phe173 in EL2. Also, it can be seen clearly that the propylphenyl ring of the compound is surrounded by hydrophobic residues Val250 in TM6 and Ile276 in TM7 mainly through the hydrophobic

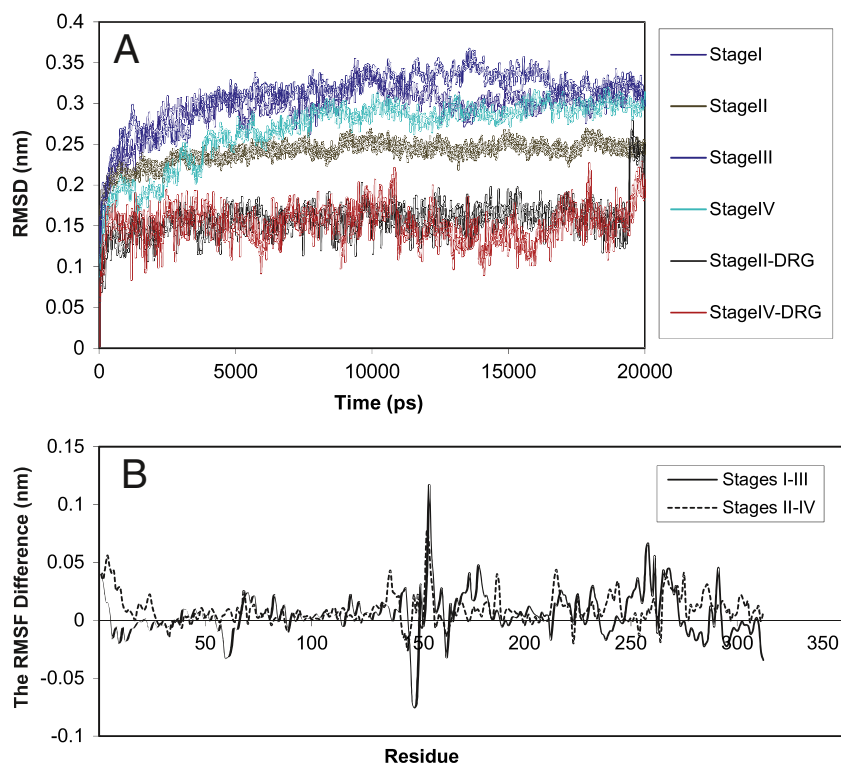
interactions. More hydrophobic interactions around this area can improve antagonist activity. In addition, the piperazinylpropylphenyl moiety of the ligand is surrounded by a hydrophobic residue (Leu172). Lys265 is observed in proximity to this moiety and the hydrophobic pocket formed by the lipophobic part of Lys265. Lys265 was unable to form an interaction with the phenyl ring of the ligand as a matter of the large distance between them. Also, there are hydrophobic interactions between the pyrrolopyrimidine moiety of the ligand and Met272 and Val11. Residues Glu174, Asn254, Asn273, Lys269 and Asn266 in this case are too far to be able to take part in any favorable interactions.

Key residues for hydrophobic interactions (Phe173, His251, Trp247, Ile276, and Val85) were consistent with mutational experiments reported in the literature [17, 30, 48], but residues for hydrogen bonding determined in this study were not in good agreement with the experimental reported results. During the docking analysis, we identified that the effective binding site of A_{2B}AR for the studied antagonist is in the upper region of transmembrane (TM) helical bundle surrounded by TMs 3, 6, 2 and ELs 1 and 2.

Molecular dynamics simulation: stage II

For further investigation of the binding site of a known potent antagonist and also to explain effects of ligand binding on the conformation of the final refined receptor, we

Fig. 1 (a) Graphical representation of RMSD of protein atoms from starting structure of $A_{2B}AR$ as a function of time during MD simulation stages I-IV as well as the RMSD of ligand's atoms relative to its original conformation from the starting structure of docked ligand as a function of time during MD simulation stages II and IV. (b) The difference of RMSF for the protein backbone of $A_{2B}AR$ during stages I-III (stage I minus III) and II-IV (stage II minus IV)



performed a second MD simulation on the ligand-receptor complex in the lipid bilayer.

The nitrogens in piperazine ring of the ligand are located close to carboxylic C=O of Glu14 (3.09 Å) and the amidic C=O of Asn273 (2.95 Å) and seem to be involved in the new hydrogen bonding with these residues (Fig. 2b). The pyrrolopyrimidine ring formed a hydrogen bond to Ser68 in the same way as what was seen in the docking results. Also, the carbonyl group of the acetamide moiety of the ligand is bonded through hydrogen bonding to the Gly70. To date, there are not mutagenesis studies to verify that residues Glu14, Gly70, Ser68 and Asn273 are involved in a hydrogen bonding interaction with $A_{2A}AR$ and $A_{2B}AR$ antagonists. Nevertheless, it has been reported in previous studies that Ser68 and Asn273 were involved in hydrogen bond formation [18, 20]. Meanwhile, Lys170 and Lys269 are involved in cation- π interactions with the phenyl and pyrrolopyrimidine moiety of the ligand.

Val85, Ala64, Ile65, Ile61, Ile276 and Thr89 form a suitable hydrophobic pocket for the phenyl ring of the ligand, although favorable hydrophobic interactions between Trp247, Val250, Phe173 and phenyl ring of the ligand disappeared. The piperazinylpropylphenyl moiety of the ligand is anchored by hydrophobic interactions with His251 and Ile172.

It is interesting that Asn254, Phe173 and Glu174 which according to the literature and site directed mutagenesis studies are present in the active site of the $A_{2B}AR$, are located far from the ligand according to the results of this stage, thus are unable to have favorable interactions with the ligand.

Based on these results, the major part of the binding site is made up by the transmembrane helices. However, the pocket of this binding site is located in the extracellular side of the trans-membrane domain and partly covered by the second extracellular loop (EL2). However, the exact structure of the second extracellular loop, which may also be involved in ligand binding, was quite uncertain to date. In this work we have made suggestions on the potential structure of this part. Our strategy to elucidate this loop is part of the next stages.

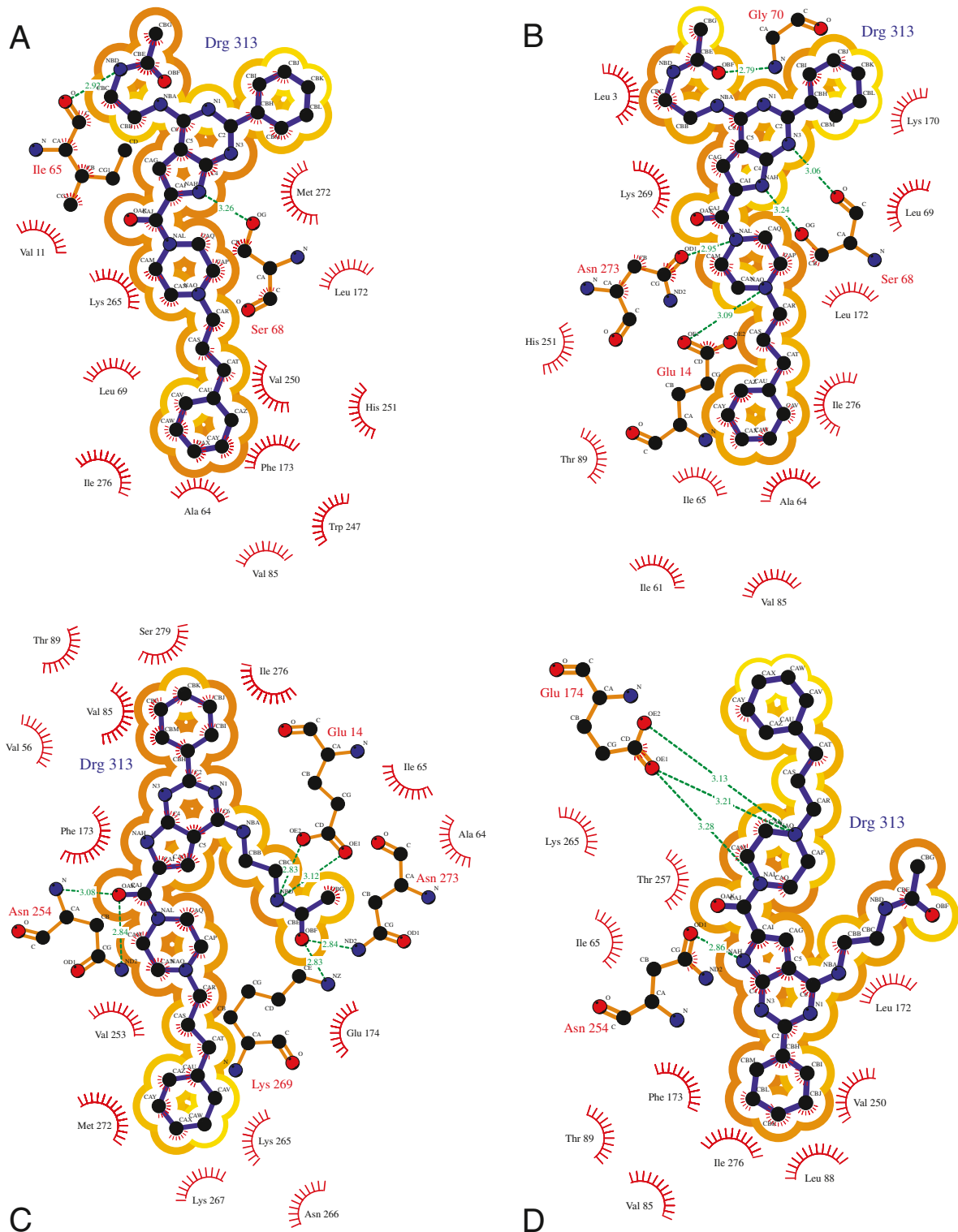
Molecular dynamics simulation: stage III

The conformational stability of the modified $A_{2B}AR$ in the simulation procedure was assessed by carrying out a 20 ns MD simulation on glycosylated and palmitoylated $A_{2B}AR$ in a lipid bilayer. The aim of this stage was to obtain a more precise receptor model in the state close to natural conditions and to further explore the binding modes of the ligand.

Many of the key residues and motif characteristics of GPCRs are also present in adenosine receptors. The followings are some of the distinguished features:

The extracellular domain of the $A_{2B}AR$ contains three extracellular loops. The second extracellular domain of the $A_{2B}AR$ includes two NXS/T (Asn-X-Ser/Thr) consensus

Fig. 2 Structure and intermolecular interactions of OSIP339391 with $A_{2B}AR$ in 2D flattened space generated by LIGPLOT after MD simulation stages I-IV. (a) Stage I. (b) Stage II. (c) Stage III. (d) Stage IV



C

Key

- Ligand bond
- Non-ligand bond
- Hydrogen bond and its length
- Solvent accessibility shading: Buried
- Solvent accessibility shading: Highly accessible
- His 53 Non-ligand residues involved in hydrophobic contact(s)
- Corresponding atoms involved in hydrophobic contact(s)

sequences for N-linked (Asn-linked) glycosylation where X is any amino acid except Pro or Asp [49]. These motifs are located at Asn153 and Asn163 on EL2 of the A_{2B}AR [11, 15, 40].

Plasma membrane glycoproteins are always oriented with the carbohydrate-bearing domain on the extracellular surface of the plasma membrane of all known cloned mammalian GPCRs. The asymmetric arrangement of membrane proteins results in functional asymmetry.

All adenosine receptor subtypes have potential N-linked glycosylation sites [15]. A_{1A}AR and A_{2A}AR have been shown to be glycosylated in vivo [50, 51]. Consensus sites for N-linked glycosylation exist on the extracellular regions of ARs, although the precise location of the sites for this PTM varies amongst the AR subtypes [52].

The cytoplasmic side contains three intracellular loops, and lipid anchoring sites that create a fourth intracellular loop. Another aspect of the interaction of lipids and proteins is that some membrane proteins are anchored to one leaflet or another of the lipid bilayer by covalent linkages to certain lipids [41]. These lipid-protein assemblies are found only on the inner face of the plasma membrane [53]. The carboxyl-terminal tails of A_{1A}AR, A_{2B}AR, and A_{3A}AR, but not A_{2A}AR, possess a conserved cysteine residue that may putatively serve as a consensus potential site for receptor palmitoylation [11, 12, 40]. The potential of these cysteine residues as sites for A₁ and A₃ palmitoylation was determined by site-directed mutagenesis [11, 54].

Like many other GPCRs, A_{2B} receptor is anchored to the cell membrane via a palmitate anchor at the C-terminus and two potential N-glycosylation sites. We performed MD simulations of the A_{2B}AR model with the two N-linked N-acetylglucosamine (at Asn153 and Asn163) and the palmitate anchor attached to Cys311 in an explicit lipid environment. The rationale was to investigate the influence of the glycosylation and the palmitate anchor on the structural and dynamical behavior of the membrane protein.

Finally, in order to investigate its binding mode, OSIP339391 was docked into the modified receptor model obtained from the MD simulation. The best possible binding mode of ligand OSIP339391 as the most biologically active compound in the A_{2B}AR active site is illustrated in Fig. 3.

The docking results showed that Asn254 form a hydrogen bonding interaction with the carbonyl group located between the pyrrolopyrimidine and piperazine moieties (Fig. 2c). Asn254 was a very important residue in mutation experiments reported in the literature [8, 17–20, 30]. The carbonyl group of the acetamide moiety of the ligand is involved in hydrogen-bonding with Asn273 and Lys269. Lys269 and Glu174 are located in proximity to the carbonyl group of the acetamide moiety of the ligand. Acetamide NH is hydrogen-bonded to the carboxy oxygen of Glu14. This implies that Glu14 and Asn273 might be directly involved

or even they trigger the receptor activation mechanisms. These residues were not recognized in previous reports. In addition, the methyl of acetamide moiety is placed in the cage formed by Ala64 and Ile65. Phenyl ring attached to the pyrrolopyrimidine in the ligand structure forms hydrophobic interactions with residues Val85 and Thr89 in TM3, Val56 in TM2 and Ile276 and Ser279 in TM7. The pyrrolopyrimidine moiety is occupied by a π - π stacking interaction with Phe173 which was in agreement with Phe168 in the A_{2A}AR crystal structure [16, 17].

The piperazinylpropylphenyl moiety of the ligand is located inside the hydrophobic pocket formed by residues such as Val253, Glu174, Asn266, Lys265, Lys267 and Met272. Additionally, the cationic side chain of Lys265 and Lys267 are involved in cation- π interaction with the propylphenyl moiety of the ligand.

As a conclusion, Asn254 in TM6, Val85 in TM3, Phe173 in EL2 and Ile276 in TM7 were identified critical to the antagonist binding. These residues were very consistent with much of the experimental evidence [17, 30, 48]. Considering the close relationship of the A_{2A} and A_{2B} adenosine receptor subtypes, the results were correlated to the mutagenesis data published for the much better characterized A_{2A} subtype. The results obtained in this study confirm the relevance of the similar identified interactions. For example, in A_{2A} receptor, mutation of Asn253 to alanine resulted in the complete loss of both agonist and antagonist binding [30], and mutation of Glu169 to alanine reduced the affinity for both antagonists and agonists [55]. However, the counterpart of this residue, Glu174 in EL2 of A_{2B}AR, was not involved in hydrogen-bonding interaction with OSIP339391. Furthermore, the important residues obtained from glycosylated and palmitoylated A_{2B}AR model in this stage were in a good agreement with experimental site-directed mutagenesis [55, 56] and the pharmacophore model provided by Cheng et al. [20].

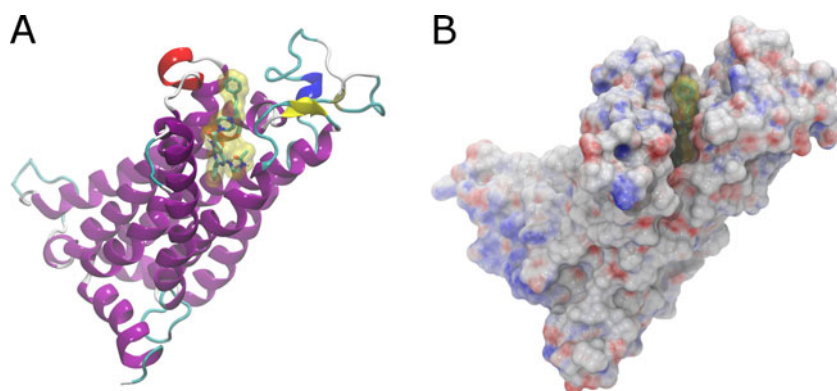
Molecular dynamics simulation: stage IV

During the 20 ns molecular dynamics simulation, the relative orientations of the ligand in A_{2B}AR in the presence of N-acetylglucosamine (GlcNAc) and S-palmitoyl resulted by conformational changes in the ligand and A_{2B} protein were explored and optimized.

A hypothetical model of the ligand-A_{2B}AR complex was obtained in a solvated phospholipid bilayer environment, starting from the initial placements based on the structural features of the docked ligand in the modified simulated A_{2B}AR model.

At the end of MD simulation, OSIP339391 showed hydrogen-bonding interactions with residues Asn254 (TM6) and Glu174 (EL2) (Fig. 2d). A π - π stacking interaction with Phe173 (EL2) and hydrophobic interactions with Val85, Thr

Fig. 3 The structure of OSIP339391 as the most potent compound in the binding cavity of $A_{2B}AR$. The ligand OSIP339391 represented by a stick model inside a solvent excluded surface (SES) in yellow, and colored by elements. (a) With a ribbon representation of the receptor colored by secondary structure elements. (b) With a SES of the receptor colored by electrostatic potential



89, Val250, Ile276 and Leu88 were observed. Conjugated hydrogen bonding from Thr257 through Glu174 and Asn254 to nitrogen atoms of piperazine and pyrrolopyrimidine rings of the ligand can interact with the carbonyl group. The simulation results demonstrated also that Lys265 is observed in the proximity of piperazinypropylphenyl moiety of the ligand and forms a hydrophobic pocket by the lipophobic part of Lys265. Lys265 may be involved in cation- π interaction with the propylphenyl moiety of the ligand. Additionally, acetamide and pyrrolopyrimidine moieties of the ligand are placed in the cage formed by Leu172. The pyrrolopyrimidine ring is stabilized by a hydrophobic interaction with Ile65. Furthermore, the ligand showed the same binding modes as the previous stage. Key binding residues were located on the EL2, TM2, TM3, TM6 and TM7. Both results were in agreement with site-directed mutagenesis experiments [17, 30, 48, 55]. These results reveal that MD simulation obligates the ligand to optimize its orientation and distance to binding site for maximum interaction with receptor. On docking of the ligand with $A_{2B}AR$, in stage III, the lowest energy conformation did not show hydrogen bonding interaction with the Glu174 due to the absence of appropriate orientation and distance. However, after MD simulation in stage IV, this kind of binding was observed.

Importantly, simulation of the modified $A_{2B}AR$ both in the presence and in the absence of ligand led to similar final peptide conformations and orientations. Therefore, we conclude that indeed the suggested docking and simulation procedure successfully produces reasonable binding modes. At the end of MD simulation position and orientation of ligand in the introduced binding site were changed and this important observation indicates useful application of MD simulations after docking of ligands in the binding site (Fig. 4).

In fact, it can be recognized that residues Phe173 and Glu174 in EL2 and Asn254 in TM6 are involved in π - π stacking and hydrogen-bonding interactions with $A_{2B}AR$ antagonist in stage IV. While, these residues were not found to be involved in ligand binding in the previously reported model constructed based on bovine rhodopsin [16]. The

same was true according to the results of stage I (except for Phe173 and Ile276) and stage II (Ile276) in the present study.

In summary, the results obtained from our findings were also in very good agreement with mutational experiments and literature reports developed by Sherbiny et al. [18].

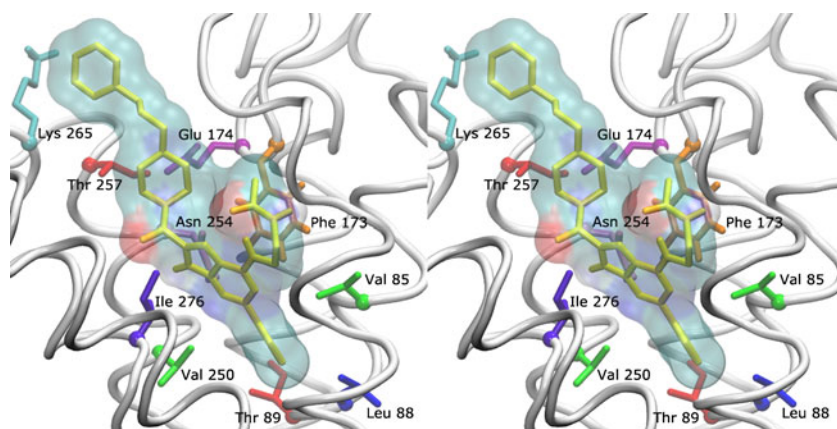
Overall analysis of MD simulations

Overall 80 ns of MD simulations were successfully carried out separately in four different stages. The physicochemical parameters such as energy for all systems reached stable values after a few hundreds of picoseconds. Systems in all stages remained stable after relaxation as no drift in energy, temperature, or lipids density was observed during the collection stage (data not shown).

RMSD of backbone atoms compared with the initial structures for stages I-IV as a function of time are shown in Fig. 1a. After 5 ns simulation, all four systems reached equilibrium and the maximal drift for all the studied structures was on the order of ~ 0.33 nm. The average RMSDs of backbone atoms in stages I-IV were 0.30 ± 0.01 , 0.25 ± 0.01 , 0.33 ± 0.01 and 0.29 ± 0.01 nm, respectively. The maximum RMSD value was ~ 0.33 nm (for backbone atom pairs), which means that somewhat larger conformational changes have taken place for stage III. Stage III shows slightly a greater backbone RMSD value than stage I (0.33 nm against 0.30 nm). This RMSD value implies that this protein structure has been slightly affected by N-acetylglucosamine (GlcNAc) and palmitoyl groups. Important hydrogen bond interactions existed in stage III, were absent in stage I. The binding modes represented in Fig. 2c and d after stages III and IV simulations are very close to the results of site directed mutagenesis and previous studies compared with the binding modes in the other stages. However, encouragingly the RMSDs of stages II and IV are significantly lower than that of stages I and III, respectively. Furthermore, independent MD simulations yield similar RMSD values, lending confidence to us of the correctness of our observations.

Moreover, RMSD values of ligand at the binding site of the investigated protein are shown in Fig. 1a. It can be seen

Fig. 4 Stereoview of the predicted binding site of A_{2B}AR after stage IV MD simulation. Compound OSIP339391 represented as yellow stick model inside a solvent excluded surface (SES) colored by elements. Important residues in the pocket are indicated by different colors (Cyan: Lys, Red: Thr, Purple: Glu, Orange: Phe, Violet: Asn, Navi: Ile, Green: Val, Blue: Leu)



that the ligand is within the active site after 2 ns in both stages (stage II and IV) with a mean RMSD values of 0.15 ± 0.02 nm and 0.16 ± 0.02 nm respectively. During the MD simulations these two modes remain in a stable binding position with low RMSD fluctuations, confirming the feasibility of the binding poses predicted by AutoDock. This is in agreement with biological activity of the ligand.

To examine the fluctuations of the structure on a residue-by-residue basis, the time averaged RMS fluctuations (RMSF) of protein backbone (N, C α , C) during the last 5 ns of the simulations were analyzed (Fig. S4). Analysis of Fig. S4 reveals that RMSFs adopt large values in the vicinity of N- and C-terminus. This behavior is attributed to the presence of loops preceding the terminal ends. Special attention was given to the regions Gln214-Thr216 (IL3), Lys147-Cys167 (EL2) and Leu258-Pro268 (EL3). These regions were more unstable than other regions of the protein during MD simulation. It was found that throughout the dynamic simulations very few fluctuations exceeded 0.1 nm and even fewer fluctuations overpassed 0.15 nm for total protein. The active site amino acids have lower RMSF values. However, comparing the RMSF plots of stages I and III, some differences can be observed. Stage III gives the model with the largest value of fluctuations showing changes inside the loops that include a significant distortion in IL3, EL3 and EL2. These results suggest that TM2-TM7 during stages II and IV bear the smallest conformational change (local RMSF of 0.12 nm). EL2 inside the receptor also exhibits almost small changes during stage IV (local RMSF of 0.15 nm).

The mobility of the equilibrated A_{2B}AR structure in the membrane was studied by computing the RMSF of the protein backbone structure versus the average equilibrated structure for the last 5 ns of the simulation. The ensemble of RMSF differences from the last 5 ns of the modified A_{2B}AR model in stage III was compared with the one of the unmodified structure in stage I (Fig. 1b). In several regions, the RMSF difference of the modified MD model is higher than that of the unmodified one. The results show several significant differences due to PTMs in stage III, where the largest

RMSF difference of the protein backbone was 0.12 nm (for EL2). It is not strange because in stage I, we focused only on the unmodified A_{2B}AR model inserted into the bilayer.

It is interesting that in stages II and IV the helical domains of A_{2B}AR exhibited relatively more fluctuations compared with stages I and III, whereas TM1, the end of TM4, the beginning of TM5 and the central parts of TM6 and TM7 reveal RMSF difference values as low as 0.04 nm. The extramembraneous domains, especially EL2, show the highest mobility as low as 0.07 nm. EL2, particularly residues 154 and 155 in this domain are very flexible. A remarkable stability of Cys311 in stage IV is found compared with stage II since this residue is not located in the binding site of the ligand.

Average number of intramolecular hydrogen bonds (shorter than 0.35 nm) and distances are calculated at different conditions for protein simulations (Table S1). All the hydrogen bonds along with the hydrophobic interactions contribute to the stability of the helices conformation. To monitor the differences in the local regions (i.e., EL2, TM8), hydrogen bonds and distances in these regions were analyzed. Hydrogen bonding between A_{2B}AR and head groups phospholipids is persistent and establishes the geometry of the protein in the bilayer. The average numbers of TM8 (Arg295-Gln312)-membrane hydrogen bonds are 12, 12, 11 and 9 for stage I, stage II, stage III and stage IV simulations, respectively. On the other hand, these characteristic numbers of TM8-TM8 hydrogen bonds are 10, 10, 13 and 12. It is promoted by the palmitoyl chain on residue Cys311. The average numbers of EL2 (Trp144-Pro178)-membrane hydrogen bonds are 4, 8, 9 and 10 for stage I, stage II, stage III and stage IV simulations, respectively. Also, for EL2-EL2 hydrogen bonds are 21, 18, 19 and 17. The portion of A_{2B}AR in the water sub phase (such as loops) can sample a much larger conformational space compared to that which is in contact with the membrane interfacial region.

Based on the structure achieved by explorative runs of molecular dynamics simulation on the complex between A_{2B}AR and the ligand, and the results of site directed

mutagenesis, some novel findings were obtained. New residues such as Thr257, Asn254 and Glu174 were positioned in proximity of the ligand and could participate in ligand-receptor interaction in stages III, IV. In stage IV, position and orientation of ligand in the binding site were changed (Fig. 4). Therefore, we deduced that structure obtained from stage IV can be used to describe ligand–receptor interactions for A_{2B}AR antagonists.

Virtual screening

To test the reliability of our model, we decided to dock some of the A_{2B} antagonists using AutoDock. It is important that the model should be able to discriminate among other A_{2B} antagonists. Molecular structures and values of the predicted and experimental binding affinities of the A_{2B} antagonists were shown in Table 1.

To demonstrate how the docking exploration was done, OSIP339391 is selected as a case study. The best scored pose (−15.12 kcal mol^{−1}) for this ligand was not the most populated cluster and also its position and orientation was not similar with the OSIP339391 at the end of stage IV simulation (Figs. 2d, 5). The next cluster (−14.28 kcal mol^{−1}) had a similar position and orientation with the reference structure and at the same time was the most populated cluster (number of neighbors=38). As a result the later one was selected. Using this method, a good correlation ($r^2=0.70$) was obtained between the experimental and predicted binding affinities of 41 docked ligands.

The binding mode of these series of ligands is conserved. Phe173 and Glu174 located in EL2 were determined to be involved in ligand-receptor interactions through π - π stacking and hydrogen bonding. Asn254 and Lys269 were crucial to form hydrogen-bonding. Ile276, Val85, Val250, Leu172,

Thr257, Thr89, Leu88 and Ile65 were found to be involved in hydrophobic interactions with the ligand. Glu14, Ser68, Asn273, Asn266, Val253, Lys265, Lys267, His251, His280 and Lys170 were proven to be in proximity of the ligand. Key binding residues were located on the EL2, TM2, TM3, TM6 and TM7. Most of these residues in the putative binding sites are conserved among the four adenosine receptor subtypes. The pocket is located in the extracellular side of the transmembrane domain and partly covered by the second extracellular loop EL2 (Figs. 3 and 5). A potential binding site of A_{2B} was verified according to the previous studies of site-directed mutagenesis [17, 30, 55, 56]. The virtual screening results show that all of the studied ligands occupy an almost similar space in the binding site. The best possible binding mode of ligand OSIP339391 as the most potent compound in the A_{2B} active site is illustrated in Fig. 5.

Discussion

It seems plausible that the conformation of EL2 and even EL3 are affected by the glycosylation due to glycosylated (Asn-X-Ser/Thr) motif existing in EL2. Furthermore, the RMSF difference analysis reveals that the more flexible residues are 155 and 147–149. These residues were affected more by the glycosylated residues 153 and 163.

In the planar state, lipids can produce a smaller lateral pressure in the headgroup region, which is directed toward the protein, due to the smaller headgroup size relative to the acyl chains. This reduction in headgroup lateral pressure can favor extension of the EL2 of A_{2B}AR into the lipid/water interface.

Ala291 (located at the end of TM7 and close to the beginning of TM8 region) and IL3 are close to Cys311.

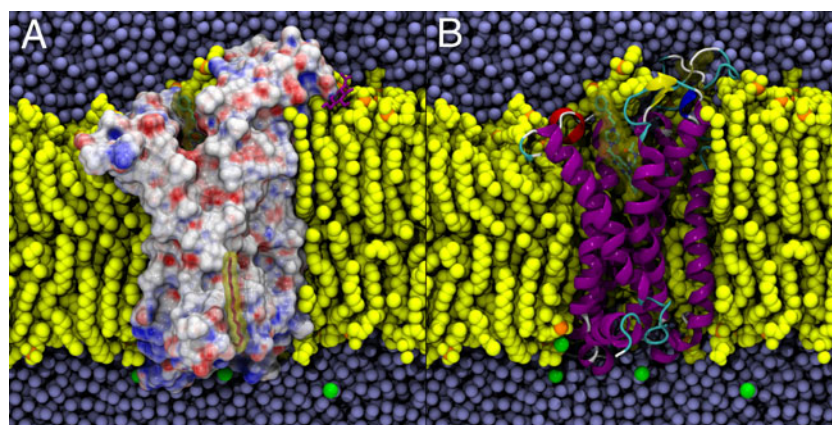


Fig. 5 A_{2B}AR –antagonist complex in hydrated POPE lipid bilayer after 20 ns MD simulation in phase IV, lipids in yellow and waters in blue. The front half of the lipid bilayer and two thirds of waters were not shown for the sake of clarity. **(a)** A_{2B}AR receptor appeared as solvent excluded surface (SES), colored by electrostatic potential.

Also, the following putative post-translational modifications are shown in violet color: glycosylation at N163, palmitoylation at C311 (with yellow SES) in the C terminus. **(b)** A_{2B}AR receptor represented as ribbon, colored by secondary structure elements

Although Cys311 is palmitoylated, the effect of this palmitoylation on them was as low as 0.04 nm. The same is true for Cys311 and Gln312 which are located in amphipathic helix TM8. On the other hand, a detailed inspection of the resulted model provided a plausible explanation for the structural changes: interactions of several residues with the phospholipid/water interface increased dramatically. The initial portion of the C-terminal tail bends toward the bilayer, leading to a deeper insertion into the bilayer. It is promoted by the palmitoyl chain on residue Cys311. This also caused a salt-bridge formation, 3.88 Å long, between Lys303 and a POP308 lipid phosphate group. Several residues away, the side chain of Lys316 also might form another salt bridge with adjacent phospholipids. Such a phenomenon cannot be attributed to residues 313–332 due to the lack of coordinate values for these positions (data not shown).

It is obvious that as palmitoylation can be viewed as an anchor for the amphipathic helix TM8, the bilayer also leads to significant deviations of this helix. The obtained hydrophobicity of palmitoylation provides the driving free energy [57]. This shows the importance of PTM in membrane protein modeling. This observation might be physiologically essential for interaction with different protein components related to sorting and signaling of A_{2B}AR.

The glycosylated domain of the modified A_{2B}AR including the binding site exhibits significant deviations and large amplitude fluctuations in contrast with palmitoylated domain. The rather substantial differences in the mobility of the structural domains of A_{2B}AR led to further analysis of its structure.

The MD simulation of the modified A_{2B}AR in a native-like membrane environment yields a significant structural rearrangement versus the unmodified structure. This phenomenon can be important for ligand binding to membrane protein (Fig. 5).

In summary, EL2 exhibits significant mobility and is very flexible, in agreement with its function as a binding site [55]. Similar rearrangements in the EL3 and IL3 and in the adjacent helices result in optimized hydrophobic and electrostatic interactions with adjacent phospholipids. In particular, Glu174 and Phe173 in EL2 slightly shift away from the bilayer toward the aqueous phase. Asn254 and Thr257 located in TM6 close to EL3 also move toward the lipid/water interface. This demonstrates that the conformations of the EL2 in the unmodified structure are not well-optimized to accommodate a ligand. The importance of these changes is due to their characteristic flexibility that they could have a role in the conformational switches of the receptor. As the results of the docking and simulations obtained from our study suggest that glycosylation changes the flexibility of some parts of the A_{2B}AR.

Many studies have been conducted in an attempt to define the precise roles of oligosaccharide chains in the

functions of glycoproteins [41]. Oligosaccharide chains may influence the sequence of polypeptide-folding events that determine the tertiary structure of the protein. Steric interactions between peptide and oligosaccharide may preclude one folding route and favor another [53]. It is mentioned in the literature that glycosylation of rhodopsin, A_{2A}AR, β₂-adrenergic, GnRH, and glycoprotein hormone receptors have no effects on ligand binding or functional activity of them [40, 58, 59], but there are some controversial reports for the role of glycosylation on ligand binding.

Rhodopsin is glycosylated at Asn2 and Asn15 [60, 61]. Experimental studies on the role of this glycosylation on rhodopsin folding and function has performed by Khorana et al. [61]. Amino acid replacements at positions 2 and 15 showed that the substitutions at Asn2 had no significant effect on the folding, cellular transport, and/or function of rhodopsin, whereas those at Asn15 caused poor folding and were defective in transport to the cell surface. These results brought the researchers to the conclusion that Asn15 glycosylation is important in signal transduction [61]. Also, another investigation into the functional role of human prostacyclin receptor glycosylation revealed effects on ligand binding, receptor activation and membrane localization [62]. The results of our study suggest that glycosylation changes the flexibility of some parts of the A_{2B} receptor. The N-acetylglucosamine moieties had influence on the overall conformational properties of A_{2B}AR.

Attachment of a specific lipid to a membrane protein has a targeting function, directing the protein to its correct membrane location [53]. Alternatively, changes in hydrophobicity imparted by palmitoylation may lead to conformational changes that result in modulation of receptor function. The obtained results in this study suggest that palmitoylation facilitates anchoring of the C-terminal portion of the cytoplasmic tail thereby creating a fourth intracellular loop.

It can be suggested that association of the membrane-water interface with the EL2 and the adjacent (Asn-X-Ser/Thr) sequence motif of A_{2B}AR can impose stress/strain on the protein, thereby affecting its function. A remarkable stability of the transmembrane (TM) helix bundle in the bilayer is found compared with the extramembraneous loops, which possibly pertains to the physiological role of the receptor. Finally, the current molecular dynamics model serves as a platform for the future structure-function studies of A_{2B}AR and other homologous GPCRs.

References

1. Martinelli A, Tuccinardi T (2008) Molecular modeling of adenosine receptors: new results and trends. *Med Res Rev* 28(2):247–277. doi:10.1002/med.20106

2. Beukers MW, Meurs I, Ijzerman AP (2006) Structure-affinity relationships of adenosine A(2B) receptor ligands. *Med Res Rev* 26(5):667–698. doi:10.1002/med.20069
3. Jacobson KA, Gao ZG (2006) Adenosine receptors as therapeutic targets. *Nat Rev Drug Discov* 5(3):247–264. doi:10.1038/nrd1983
4. Aherne CM, Kewley EM, Eltzschig HK (2011) The resurgence of A2B adenosine receptor signaling. *Biochim Biophys Acta Biomembranes* 1808(5):1329–1339. doi:10.1016/j.bbame.2010.05.016
5. Palczewski K (2006) G protein-coupled receptor rhodopsin. *Annu Rev Biochem* 75:743–767. doi:10.1146/annurev.biochem.75.103004.142743
6. Blom N, Sicheritz-Ponten T, Gupta R, Gammeltoft S, Brunak S (2004) Prediction of post-translational glycosylation and phosphorylation of proteins from the amino acid sequence. *Proteomics* 4(6):1633–1649. doi:10.1002/pmic.200300771
7. Vauquelin G, Bv M (2007) G protein-coupled receptors: molecular pharmacology from academic concept to pharmaceutical research. Wiley, Chichester
8. Katritch V, Kufareva I, Abagyan R (2011) Structure based prediction of subtype-selectivity for adenosine receptor antagonists. *Neuropharmacology* 60(1):108–115. doi:10.1016/j.neuropharm.2010.07.009
9. Palczewski K, Kumasaka T, Hori T, Behnke CA, Motoshima H, Fox BA, Le Trong I, Teller DC, Okada T, Stenkamp RE, Yamamoto M, Miyano M (2000) Crystal structure of rhodopsin: a G protein-coupled receptor. *Science* 289(5480):739–745
10. Qanbar R, Bouvier M (2003) Role of palmitoylation/depalmitoylation reactions in G-protein-coupled receptor function. *Pharmacol Ther* 97(1):1–33
11. Gao ZH, Ni YJ, Szabo G, Linden J (1999) Palmitoylation of the recombinant human A(1) adenosine receptor: enhanced proteolysis of palmitoylation-deficient mutant receptors. *Biochem J* 342:387–395
12. Olah ME, Stiles GL (2000) The role of receptor structure in determining adenosine receptor activity. *Pharmacol Ther* 85(2):55–75
13. Ulloa-Aguirre A, Stanislaus D, Janovick JA, Conn PM (1999) Structure-activity relationships of G protein-coupled receptors. *Arch Med Res* 30(6):420–435
14. Jenkins N, Curling EMA (1994) Glycosylation of recombinant proteins - problems and prospects. *Enz Microb Technol* 16(5):354–364
15. Iismaa TP, Biden TJ, Shine J (1995) G protein-coupled receptors. RG Landes, Austin
16. Ivanov AA, Baskin II, Palyulin VA, Piccagli L, Baraldi PG, Zefirov NS (2005) Molecular Modeling and molecular dynamics simulation of the human A(2B) adenosine receptor. The study of the possible binding modes of the A(2B) receptor antagonists. *J Med Chem* 48(22):6813–6820. doi:10.1021/jm049418o
17. Jaakola VP, Griffith MT, Hanson MA, Cherezov V, Chien EYT, Lane JR, Ijzerman AP, Stevens RC (2008) The 2.6 angstrom crystal structure of a human A(2A) adenosine receptor bound to an antagonist. *Science* 322(5905):1211–1217. doi:10.1126/science.1164772
18. Sherbiny FF, Schiedel AC, Maass A, Muller C (2009) Homology modelling of the human adenosine A(2B) receptor based on X-ray structures of bovine rhodopsin, the beta(2)-adrenergic receptor and the human adenosine A(2A) receptor. *J Comput Aided Mol Des* 23(11):807–828. doi:10.1007/s10822-009-9299-7
19. Goddard WA, Kim SK, Li YY, Trzaskowski B, Griffith AR, Abrol R (2010) Predicted 3D structures for adenosine receptors bound to ligands: comparison to the crystal structure. *J Struct Biol* 170(1):10–20. doi:10.1016/j.jsb.2010.01.001
20. Cheng FX, Xu ZJ, Liu GX, Tang Y (2010) Insights into binding modes of adenosine A(2B) antagonists with ligand-based and receptor-based methods. *Europ J Med Chem* 45(8):3459–3471. doi:10.1016/j.ejmech.2010.04.039
21. Rodríguez d, Piñeiro AN, Gutiérrez-de-Terán H (2011) Molecular dynamics simulations reveal insights into key structural elements of adenosine receptors. *Biochemistry* 50(19):4194–4208. doi:10.1021/bi200100t
22. Stewart M, Steinig AG, Ma CL, Song JP, McKibben B, Castelhan AL, MacLennan SJ (2004) H-3 OSIP339391, a selective, novel, and high affinity antagonist radioligand for adenosine A_{2B} receptors. *Biochem Pharmacol* 68(2):305–312. doi:10.1016/j.bcp.2004.03.026
23. Altschul SF, Madden TL, Schaffer AA, Zhang JH, Zhang Z, Miller W, Lipman DJ (1997) Gapped BLAST and PSI-BLAST: a new generation of protein database search programs. *Nucleic Acids Res* 25(17):3389–3402
24. Sali A, Blundell TL (1993) Comparative protein modeling by satisfaction of spatial restraints. *J Mol Biol* 234(3):779–815
25. Fiser A, Do RKG, Šali A (2000) Modeling of loops in protein structures. *Protein Sci* 9(9):1753–1773. doi:10.1110/ps.9.9.1753
26. Shen MY, Sali A (2006) Statistical potential for assessment and prediction of protein structures. *Protein Sci* 15(11):2507–2524. doi:10.1110/ps.062416606
27. Laskowski RA, Macarthur MW, Moss DS, Thornton JM (1993) PROCHECK - A program to check the stereochemical quality of protein structures. *J Appl Crystallogr* 26:283–291
28. Luthy R, Bowie JU, Eisenberg D (1992) Assessment of protein models with 3-dimensional profiles. *Nature* 356(6364):83–85
29. Morris GM, Goodsell DS, Halliday RS, Huey R, Hart WE, Belew RK, Olson AJ (1998) Automated docking using a Lamarckian genetic algorithm and an empirical binding free energy function. *J Comput Chem* 19(14):1639–1662
30. Kim JH, Wess J, Vanrhee AM, Schoneberg T, Jacobson KA (1995) Site-directed mutagenesis identifies residues involved in ligand recognition in the human A_{2A} adenosine receptor. *J Biol Chem* 270(23):13987–13997
31. Wallace AC, Laskowski RA, Thornton JM (1995) LIGPLOT - A program to generate schematic diagrams of protein ligand interactions. *Protein Eng* 8(2):127–134
32. Van der Spoel D, Lindahl E, Hess B, Groenhof G, Mark AE, Berendsen HJC (2005) GROMACS: Fast, flexible, and free. *J Comput Chem* 26(16):1701–1718. doi:10.1002/jcc.20291
33. Tieleman DP, MacCallum JL, Ash WL, Kandt C, Xu ZT, Monticelli L (2006) Membrane protein simulations with a united-atom lipid and all-atom protein model: lipid-protein interactions, side chain transfer free energies and model proteins. *J Phys Condens Matter* 18(28):S1221–S1234. doi:10.1088/0953-8984/18/28/s07
34. Humphrey W, Dalke A, Schulten K (1996) VMD: Visual molecular dynamics. *J Mol Graph* 14(1):33
35. Rivaill L, Chipot C, Maigret B, Bestel I, Sicsic S, Tarek M (2007) Large-scale molecular dynamics of a G protein-coupled receptor, the human 5-HT₄ serotonin receptor, in a lipid bilayer. *J Mol Struct (THEOCHEM)* 817(1–3):19–26. doi:10.1016/j.theochem.2007.04.012
36. Berendsen HJC, Postma JPM, van Gunsteren WF, Dinola A, Haak JR (1984) Molecular-dynamics with coupling to an external bath. *J Chem Phys* 81(8):3684–3690
37. Darden T, York D, Pedersen L (1993) Particle mesh Ewald - An N·Log(N) method for Ewald sums in large systems. *J Chem Phys* 98(12):10089–10092
38. Hess B, Bekker H, Berendsen HJC, Fraaije J (1997) LINCS: a linear constraint solver for molecular simulations. *J Comput Chem* 18(12):1463–1472
39. van Aalten DMF, Bywater R, Findlay JBC, Hendlich M, Hooft RWW, Vriend G (1996) PRODRG, a program for generating molecular topologies and unique molecular descriptors from coordinates of small molecules. *J Comput Aided Mol Des* 10(3):255–262
40. Piirainen H, Ashok Y, Nanekar RT, Jaakola VP (2011) Structural features of adenosine receptors: from crystal to function. *Biochim*

- Biophys Acta Biomembranes 1808(5):1233–1244. doi:10.1016/j.bbamem.2010.05.021
41. Murray RK, Granner DK, Rodwell VW (2006) Harper's illustrated biochemistry. 27th edn. In: Murray RK, Granner DK, Rodwell VW (eds) Lange medical books. McGraw-Hill, New York
 42. Gheidi M, Safari N, Bahrami H, Zahedi M (2007) Theoretical investigations of the hydrolysis pathway of verdoheme to biliverdin. *J Inorg Biochem* 101(3):385–395. doi:10.1016/j.jinorgbio.2006.10.012
 43. Stefanachi A, Brea JM, Cadavid MI, Centeno NB, Esteve C, Loza MI, Martinez A, Nieto R, Raviña E, Sanz F, Segarra V, Sotelo E, Vidal B, Carotti A (2008) 1-, 3- and 8-substituted-9-deazaxanthines as potent and selective antagonists at the human A2B adenosine receptor. *Bioorg Med Chem* 16(6):2852–2869
 44. Baraldi PG, Tabrizi MA, Gessi S, Borea PA (2008) Adenosine receptor antagonists: Translating medicinal chemistry and pharmacology into clinical utility. *Chem Rev* 108(1):238–263
 45. Wu BL, Chien EYT, Mol CD, Fenalti G, Liu W, Katritch V, Abagyan R, Brooun A, Wells P, Bi FC, Hamel DJ, Kuhn P, Handel TM, Cherezov V, Stevens RC (2010) Structures of the CXCR4 Chemokine GPCR with small-molecule and cyclic peptide antagonists. *Science* 330(6007):1066–1071. doi:10.1126/science.1194396
 46. Bockaert J, Pin JP (1999) Molecular tinkering of G protein-coupled receptors: an evolutionary success. *EMBO J* 18(7):1723–1729
 47. Ivetac A, Sansom MSP (2008) Molecular dynamics simulations and membrane protein structure quality. *Eur Biophys J Biophys Lett* 37(4):403–409. doi:10.1007/s00249-007-0225-4
 48. Jiang QL, Lee BX, Glashofer M, van Rhee AM, Jacobson KA (1997) Mutagenesis reveals structure-activity parallels between human A(2A) adenosine receptors and biogenic amine G protein-coupled receptors. *J Med Chem* 40(16):2588–2595
 49. Rands E, Candelore MR, Cheung AH, Hill WS, Strader CD, Dixon RAF (1990) Mutational analysis of beta-adrenergic-receptor glycosylation. *J Biol Chem* 265(18):10759–10764
 50. Olah ME, Jacobson KA, Stiles GL (1990) Purification and characterization of bovine cerebral-cortex A1 adenosine receptor. *Arch Biochem Biophys* 283(2):440–446
 51. Barrington WW, Jacobson KA, Stiles GL (1990) Glycoprotein nature of the A2-adenosine receptor-binding subunit. *Mol Pharmacol* 38(2):177–183
 52. Tucker AL, Linden J (1993) Cloned receptors and cardiovascular-responses to adenosine. *Cardiovasc Res* 27(1):62–67
 53. Lehninger AL, Lehninger ALPob, Nelson DL, Cox MM (2000) In: Nelson DL, Cox MM (eds) Lehninger principles of biochemistry, 3rd edn. Worth, New York
 54. Palmer TM, Stiles GL (2000) Identification of threonine residues controlling the agonist-dependent phosphorylation and desensitization of the rat A(3) adenosine receptor. *Mol Pharmacol* 57(3):539–545
 55. Kim JH, Jiang QL, Glashofer M, Yehle S, Wess J, Jacobson KA (1996) Glutamate residues in the second extracellular loop of the human A(2a) adenosine receptor are required for ligand recognition. *Mol Pharmacol* 49(4):683–691
 56. Kim SK, Gao ZG, Van Rompaey P, Gross AS, Chen A, Van Calenbergh S, Jacobson KA (2003) Modeling the adenosine receptors: comparison of the binding domains of A(2A) agonists and antagonists. *J Med Chem* 46(23):4847–4859. doi:10.1021/jm0300431
 57. White SH, Wimley WC (1999) Membrane protein folding and stability: Physical principles. *Annu Rev Biophys Biomol Struct* 28:319–365
 58. Schoneberg T, Schulz A, Gudermann T (2002) The structural basis of G-protein-coupled receptor function and dysfunction in human diseases. In: Reviews of physiology biochemistry and pharmacology, vol 144. Springer, Berlin, pp 143–227
 59. Piersen CE, True CD, Wells JN (1994) A carboxyl-terminally truncated mutant and nonglycosylated A_{2A} adenosine receptors retain ligand-binding. *Mol Pharmacol* 45(5):861–870
 60. Huber T, Botelho AV, Beyer K, Brown MF (2004) Membrane model for the G-protein-coupled receptor rhodopsin: hydrophobic interface and dynamical structure. *Biophys J* 86(4):2078–2100
 61. Kaushal S, Ridge KD, Khorana HG (1994) Structure and function in rhodopsin - the role of asparagine-linked glycosylation. *Proc Natl Acad Sci USA* 91(9):4024–4028
 62. Stitham J, Arehart EJ, Gleim SR, Douville KL, Hwa J (2007) Human prostacyclin receptor structure and function from naturally-occurring and synthetic mutations. *Prostaglandins Other Lipid Mediat* 82(1–4):95–108. doi:10.1016/j.prostaglandins.2006.05.010